chemosensors

MDPI

Supplementary Materials

Fluorescent Calix[4]arene-Carbazole-Containing Polymers as Sensors for Nitroaromatic Explosives

Patrícia D. Barata and José V. Prata

Table of Contents

Synthesis and structural characterisation data of Calix-PPE-CBZs

Calix-PPE-CBZs were prepared by our reported procedure [1]. Some experimental details of their synthesis (Scheme S1), as well as the most relevant analytical data regarding to their structure, are partially reproduced below from reference 1.

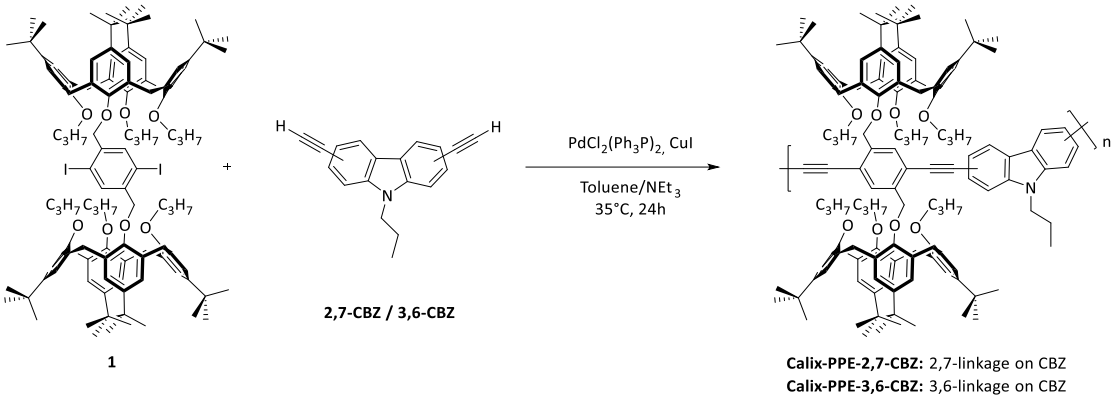

Scheme S1. Cross-coupling of bis-calix[4]arene **1** with 3,6-diethynyl-9-propyl-9*H*-carbazole and 2,7-diethynyl-9-propyl-9*H*-carbazole [1].

Calix-PPE-2,7-CBZ: To an argon degassed solution containing 100 mg (52.5 μmol) of bis-calix[4]arene **1** in dry toluene (2.1 ml) and freshly distilled NEt_3 (2.1 ml) were added $PdCl_2(PPh_3)_2$ (2.58 mg, 3.68 μmol), CuI (0.70 mg, 3.68 μmol) and 2,7-diethynyl-9-propyl-9*H*-carbazole (2,7-CBZ; 7.43 mg, 57.8 μmol) under argon. After degassing, the mixture was stirred in a pre-heated bath at 35 °C for 24 h. Solvents were removed by evaporation and the residue taken in CH_2Cl_2 and washed successively with aqueous solutions of 2% HCl, 0.1M $NaHSO_3$, 10% NH_4SCN and water. The organic extract was dried and evaporated to dryness. The residue was dissolved in a minimum amount of CH_2Cl_2 and the polymer precipitated by the addition of MeOH (2 cycles). The product was obtained as a bright yellow solid in 84.3 mg (84.1%); ν_{max}/cm^{-1} (film) 3046, 2962, 2936, 2904, 2875, 2209, 2145, 2075, 1625, 1601, 1584, 1481, 1462, 1386, 1362, 1202, 1123, 1045, 1010, 969, 887, 871, 760; λ_{max}/nm (ε_{max} x 10^{-4} $M^{-1}cm^{-1}$) 394 (6.73), 414 (6.61); δ_H/ppm ($CDCl_3$; 400 MHz) 0.75-0.92 (48H, m, C(C<u>H</u>$_3$)$_3$ (36H) and -CH_2C<u>H</u>$_3$ (12H)), 0.92-1.09 (9H, m, -*O*-CH_2CH_2C<u>H</u>$_3$ (6H) and -*N*-CH_2CH_2C<u>H</u>$_3$ (3H)), 1.16-1.35 (36H, m, C(C<u>H</u>$_3$)$_3$), 1.76-2.13 (14H, m, -*O*-CH_2C<u>H</u>$_2CH_3$ (12H) and -*N*-CH_2C<u>H</u>$_2CH_3$ (2H)), 2.98-3.30 (8H, m, ArC<u>H</u>$_2$Ar), 3.55-3.77 (4H, m, -*O*-C<u>H</u>$_2CH_2CH_3$), 3.87-4.12 (8H, m, -*O*-C<u>H</u>$_2CH_2CH_3$), 4.12-4.32 (2H, m, -*N*-C<u>H</u>$_2CH_2CH_3$), 4.33-4.80 (8H, m, ArC<u>H</u>$_2$Ar), 4.90, 5.07, 5.15 (4H, bs, ArOC<u>H</u>$_2$Ar; ratio ~1:1:4), 6.40-6.64 (8H, m, calix-Ar<u>H</u>), 6.92-7.13 (8H, m, calix-Ar<u>H</u>), 7.30-7.40 (2H, m, ArC$_{(3,6)}$<u>H</u> (carbazole); partially overlapped), 7.48-7.60 (2H, m, ArC$_{(1,8)}$<u>H</u> (carbazole)), 7.90, 8.06, 8.25 [2H, bs, *orto*-<u>H</u>-ArI (chain ends), <u>H</u>-Ar(-C≡C-)$_2$-<u>H</u> (middle chain) and *meta*-<u>H</u>-ArI (chain ends), respectively; ratio ~1:4:1; central resonance partially overlapped], 7.93-8.13 (2H, m, ArC$_{(4,5)}$<u>H</u> (carbazole); partially overlapped); δ/ppm (CD_2Cl_2; 100 MHz) 10.42, 11.05, 12.12, 23.74, 23.80, 24.12, 31.59, 31.62, 32.02, 34.12, 34.16, 34.44, 45.35, 75.61, 77.32, 77.96, 87.65, 96.57, 112.66, 120.94, 121.13, 123.23, 123.96, 123.70, 125.13, 125.41, 125.89, 125.97, 133.11, 133.29, 135.80, 135.97, 134.88, 139.64, 141.39, 144.50, 145.04, 153.06, 153.56, 155.13 (see ^{13}C assignments in reference 1). ^{13}C-^1H HSQC, ^{13}C-^1H HMBC, COSY and NOESY NMR experiments (CD_2Cl_2) were used for the ^1H/^{13}C spectral assignments (see reference 1 for details). Anal. Calcd. for $(C_{133}H_{165}NO_8)_n$: C, 83.82; H, 8.73; N, 0.73. Found: C, 79.22; H, 7.81; N, 1.03.

Calix-PPE-3,6-CBZ: The above procedure, using identical molar amounts, was applied to the synthesis of the title polymer, using 3,6-diethynyl-9-propyl-9*H*-carbazole (3,6-CBZ) as comonomer, affording 70.03 mg (69.8%) of Calix-PPE-3,6-CBZ as a light yellow solid; ν_{max}/cm^{-1} (film) 3046, 2962, 2936, 2904, 2875, 2209, 2143, 2075, 1628, 1600, 1583, 1481, 1464, 1385, 1362, 1201, 1123, 1044, 1009, 969, 883, 871, 806, 741; λ_{max}/nm (ε_{max} x 10^{-4} $M^{-1}cm^{-1}$) 318 (5.04), 361 (5.17), 380 (sh, 4.17); δ_H/ppm ($CDCl_3$; 400

MHz) 0.72-0.92 (48H, m, C(C<u>H</u>$_3$)$_3$ (36H) and -CH$_2$C<u>H</u>$_3$ (12H)), 0.93-1.06 (9H, m, -*O*-CH$_2$CH$_2$C<u>H</u>$_3$ (6H) and -*N*-CH$_2$CH$_2$C<u>H</u>$_3$ (3H)), 1.17-1.34 (36H, m, C(C<u>H</u>$_3$)$_3$), 1.75-2.10 (14H, m, -*O*-CH$_2$C<u>H</u>$_2$CH$_3$ (12H) and -*N*-CH$_2$C<u>H</u>$_2$CH$_3$ (2H)), 3.00-3.26 (8H, m, ArC<u>H</u>$_2$Ar), 3.55-3.71 (4H, m, -*O*-C<u>H</u>$_2$CH$_2$CH$_3$), 3.84-4.10 (8H, m, -*O*-C<u>H</u>$_2$CH$_2$CH$_3$), 4.20-4.33 (2H, m, -*N*-C<u>H</u>$_2$CH$_2$CH$_3$), 4.34-4.48 (4H, m, ArC<u>H</u>$_2$Ar), 4.50-4.75 (4H, m, ArC<u>H</u>$_2$Ar), 4.84-4.91, 5.02-5.08, 5.08-5.20 (4H, m, ArOC<u>H</u>$_2$Ar; ratio ~1:1:2), 6.42-6.58 (8H, m, calix-Ar<u>H</u>), 6.93-7.11 (8H, m, calix-Ar<u>H</u>), 7.30-7.42 (2H, m, Ar<u>H</u> (carbazole)), 7.54-7.63 (2H, m, Ar<u>H</u> (carbazole)), 7.87-7.92, 7.99-8.07, 8.24-8.28 (2H, m, Ar<u>H</u>; partially overlapped), 8.16-8.30 (2H, m, Ar<u>H</u> (carbazole); partially overlapped); δc/ppm (CD$_2$Cl$_2$; 100 MHz) 10.41, 11.09, 12.04, 22.87, 23.77, 24.10, 31.60, 32.02, 34.09, 34.40, 45.49, 75.60, 77.21, 77.29, 77.97, 87.00, 96.30, 109.70, 114.40, 114.61, 122.81, 122.97, 125.07, 125.36, 125.90, 125.96, 130.76, 133.00, 133.06, 135.25, 135.94, 134.81, 141.26, 141.60, 144.42, 144.93, 153.50, 153.53, 155.17 (see ^{13}C assignments in reference 1). ^{13}C-^{1}H HSQC, ^{13}C-^{1}H HMBC, COSY and NOESY NMR experiments (CD$_2$Cl$_2$) were used for the ^{1}H/^{13}C spectral assignments (see reference 1 for details). Anal. Calcd. for (C$_{133}$H$_{165}$NO$_8$)$_n$: C, 83.82; H, 8.73; N, 0.73. Found: C, 79.11; H, 7.78; N, 0.95.

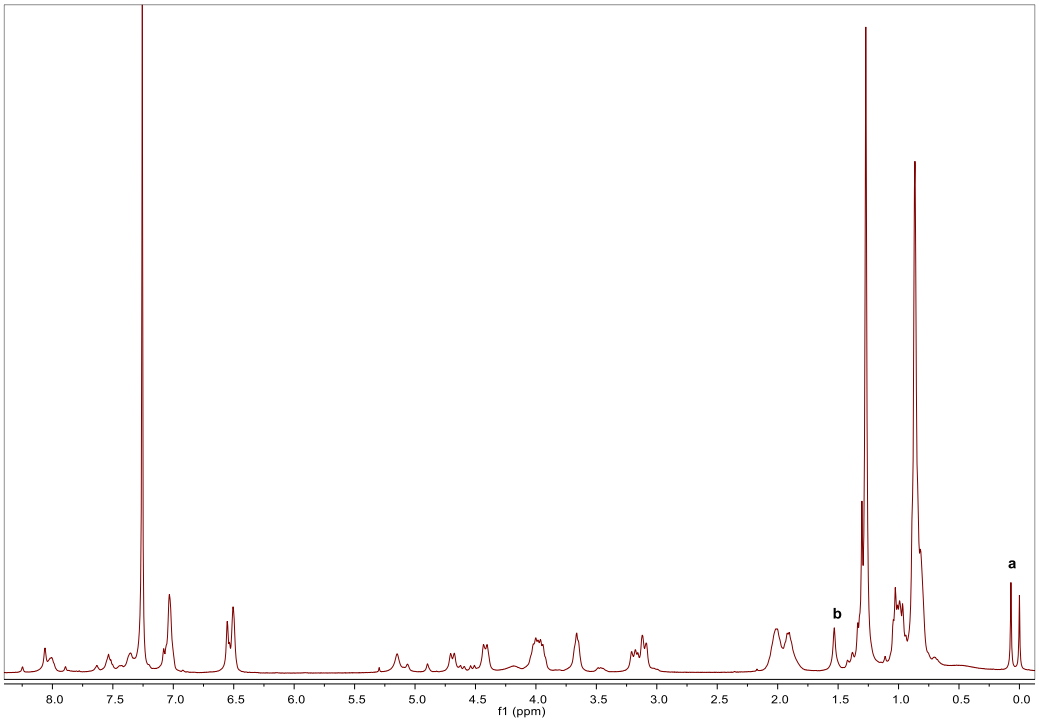

Figure S1. ^{1}H NMR spectrum of Calix-PPE-2,7-CBZ in CDCl$_3$ (400 MHz, 25 °C); [a]silicone grease; [b]water.

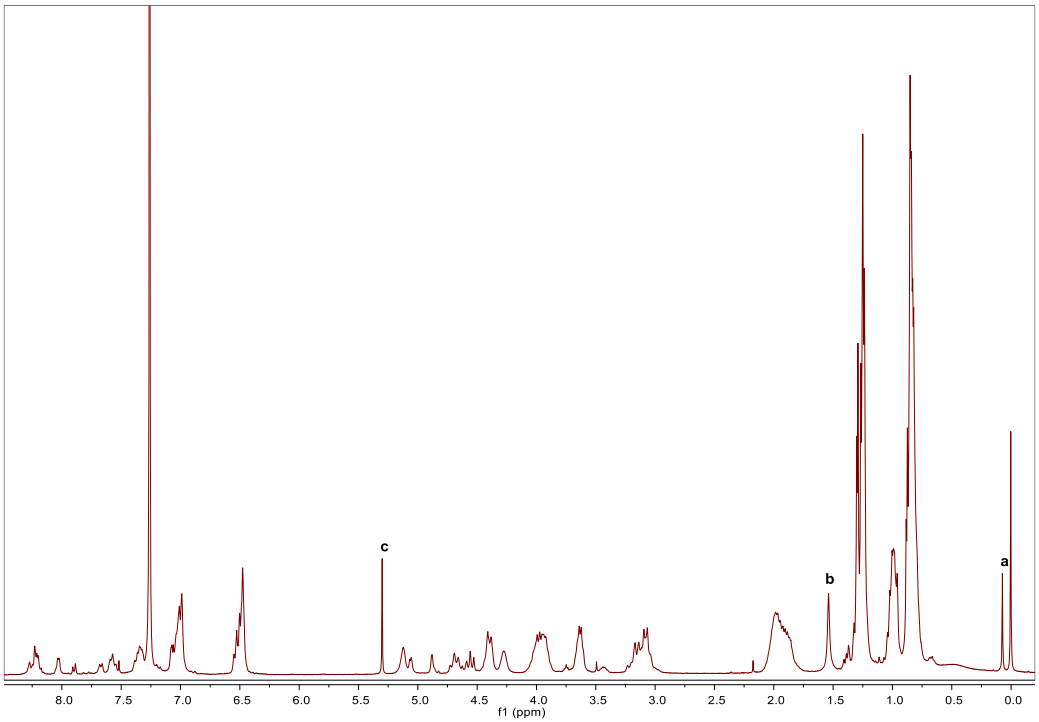

Figure S2. ^{1}H NMR spectrum of Calix-PPE-3,6-CBZ in $CDCl_3$ (400 MHz, 25 °C); [a]silicone grease; [b]water; [c]CH_2Cl_2.

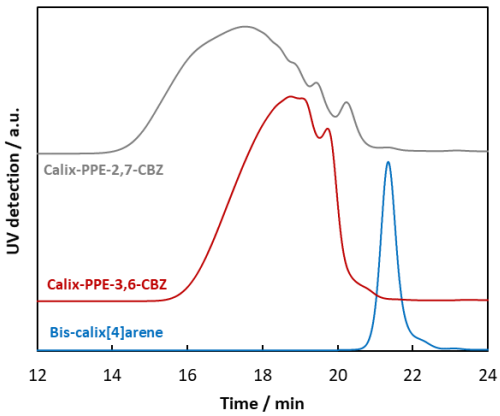

Figure S3. GPC traces of isolated Calix-PPE-CBZs and bis-calix[4]arene **1** against monodisperse polystyrene standards (THF as eluent at 35 °C).

Calix-PPE-2,7-CBZ: M_w = 26,700 g mol^{-1}; M_w/M_n = 2.99; average DP = 5.

Calix-PPE-3,6-CBZ: M_w=7,660 g mol^{-1}; M_w/M_n = 1.73; average DP = 2.

Computational studies

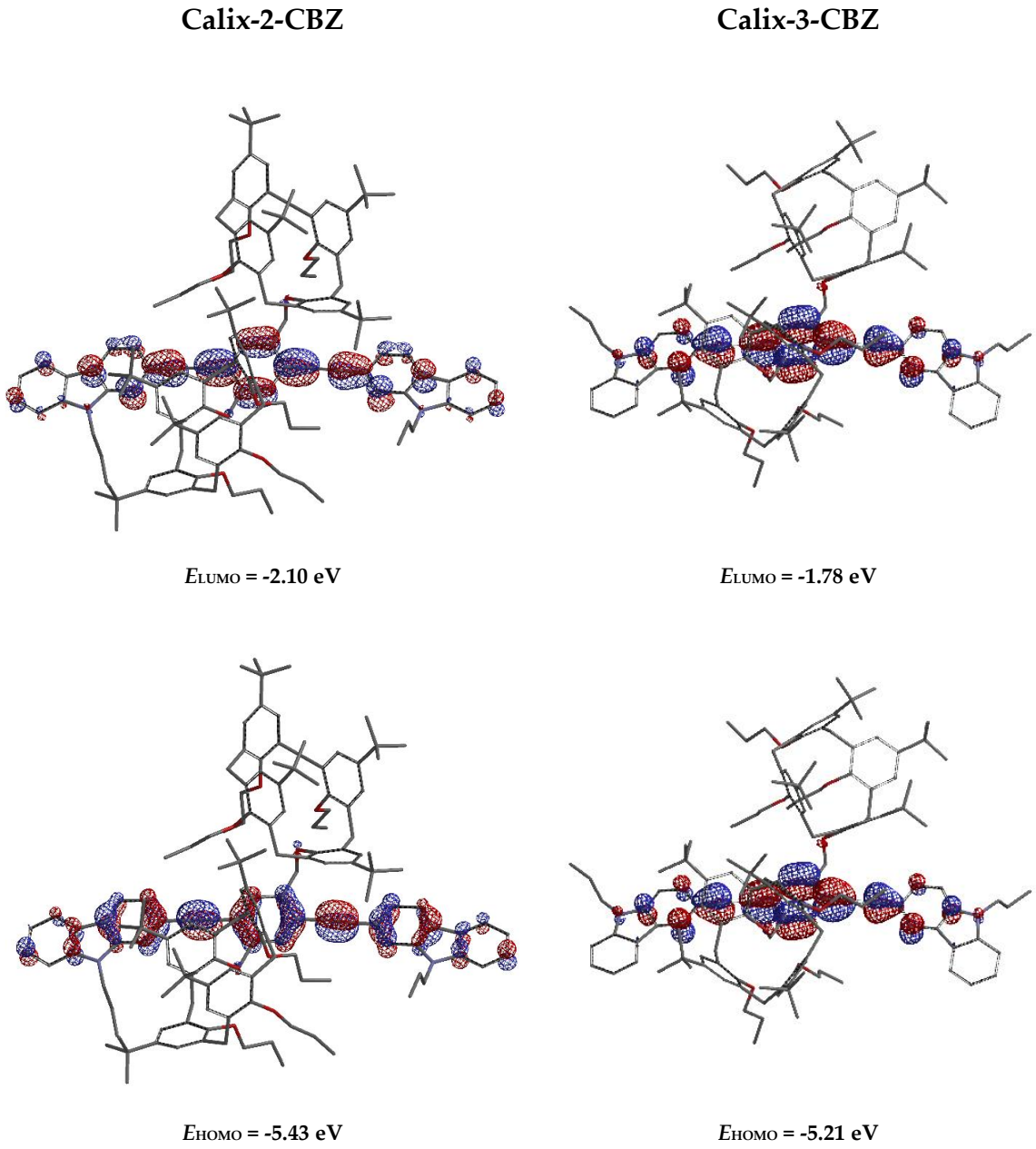

Figure S4. HOMO and LUMO mapped on optimised structures of Calix-2-CBZ and Calix-3-CBZ. DFT calculations run at the B3LYP-D3/6-311+G(d,p) level of theory in vacuum [2,3]. Hydrogens omitted for clarity.

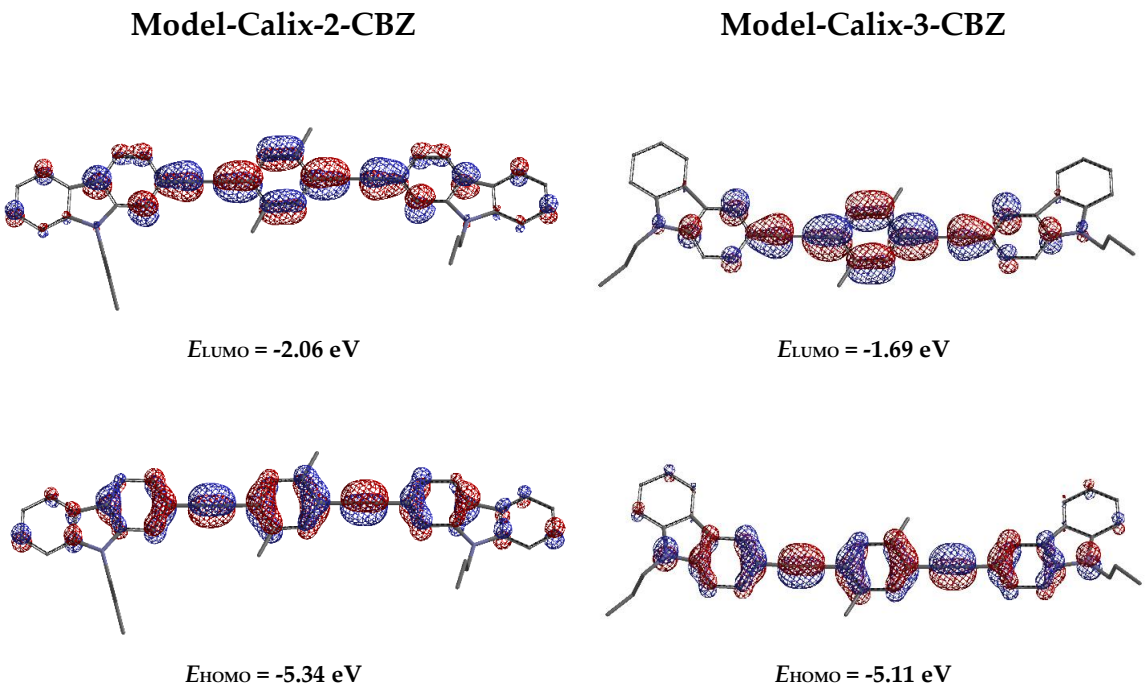

Figure S5. HOMO and LUMO mapped on optimised structures of Model-Calix-CBZs. DFT calculations run at the B3LYP-D3/6-311+G(d,p) level of theory in vacuum [2,3]. Hydrogens omitted for clarity.

Pentamer model-Calix-PPE-2,7-CBZ

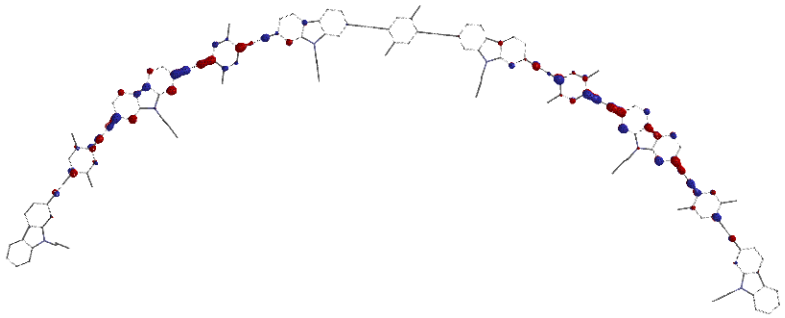

E_{LUMO+1} = **-2.29 eV**

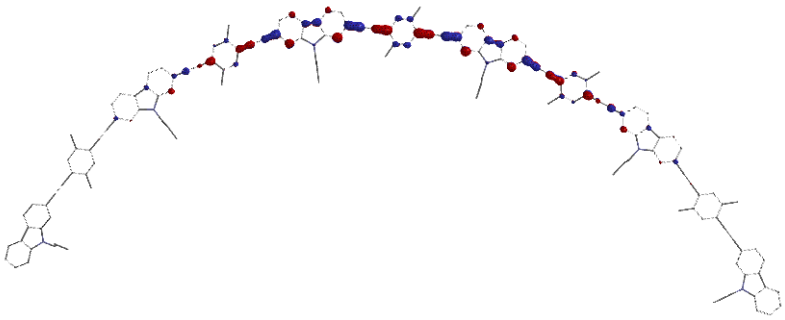

E_{LUMO} = **-2.39 eV**

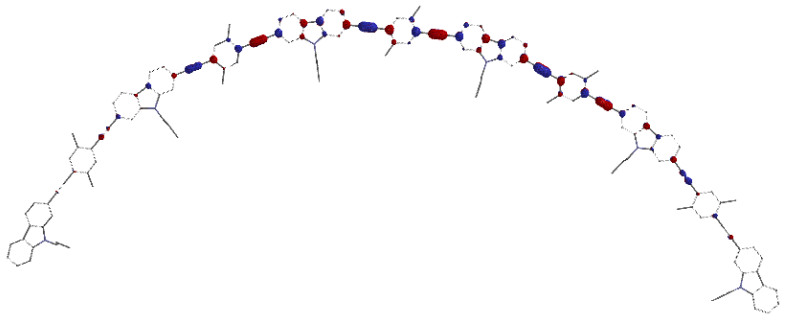

E_{HOMO} = **-5.22 eV**

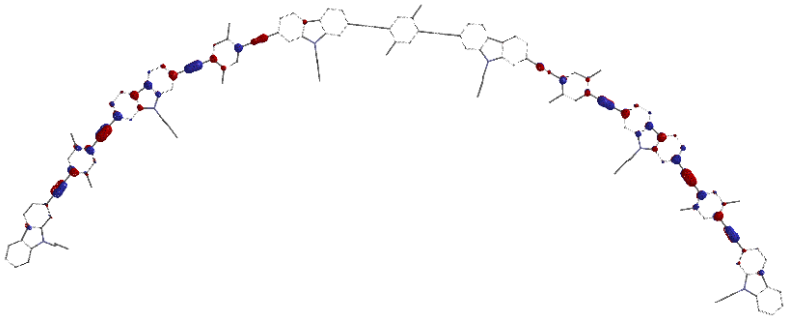

E_{HOMO-1} = **-5.29 eV**

Figure S6. Molecular orbitals ($HOMO_{-1}$, HOMO, LUMO and $LUMO_{+1}$) mapped on optimised structures of Pentamer model-Calix-PPE-2,7-CBZ. DFT calculations run at the B3LYP-D3/6-311+G(d,p) level of theory in vacuum [2,3]. Hydrogens omitted for clarity.

Pentamer model-Calix-PPE-3,6-CBZ

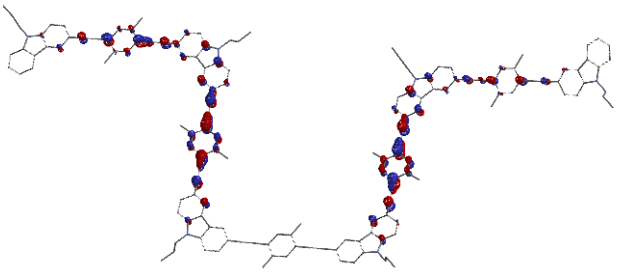

E_{LUMO+1} = **-1.81 eV**

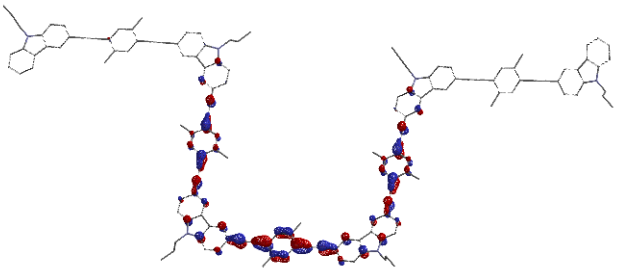

E_{LUMO} = **-1.87 eV**

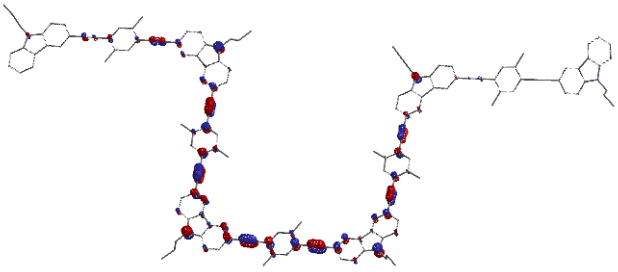

E_{HOMO} = **-5.06 eV**

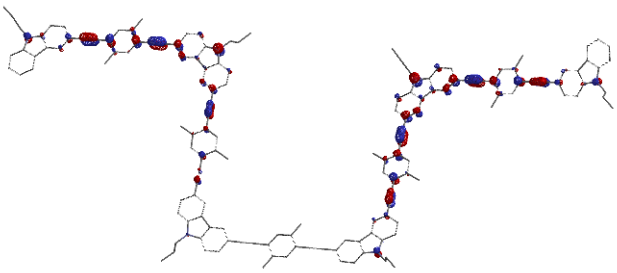

E_{HOMO-1} = **-5.10 eV**

Figure S7. Molecular orbitals (HOMO$_{-1}$, HOMO, LUMO and LUMO$_{+1}$) mapped on optimised structures of Pentamer model-Calix-PPE-3,6-CBZ. DFT calculations run at the B3LYP-D3/6-311+G(d,p) level of theory in vacuum [2,3]. Hydrogens omitted for clarity.

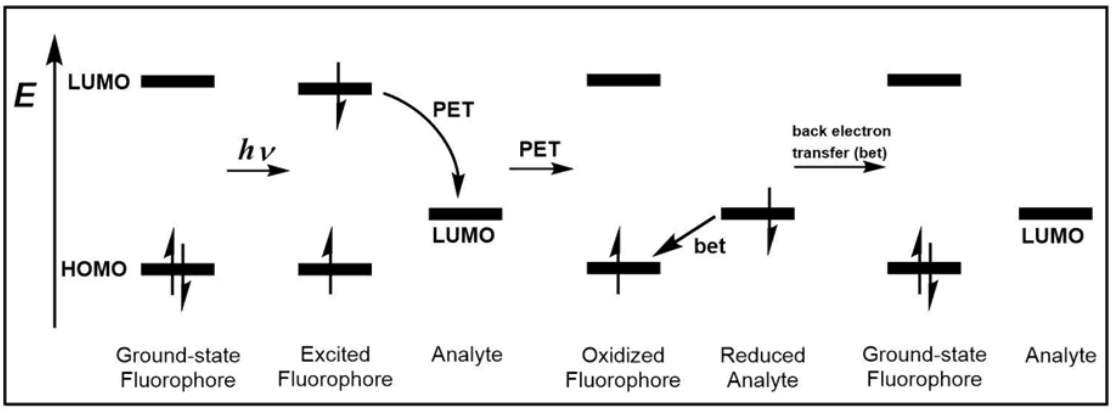

Figure S8. Illustration of the mechanism of oxidative fluorescence quenching by photoinduced electron transfer (PET).

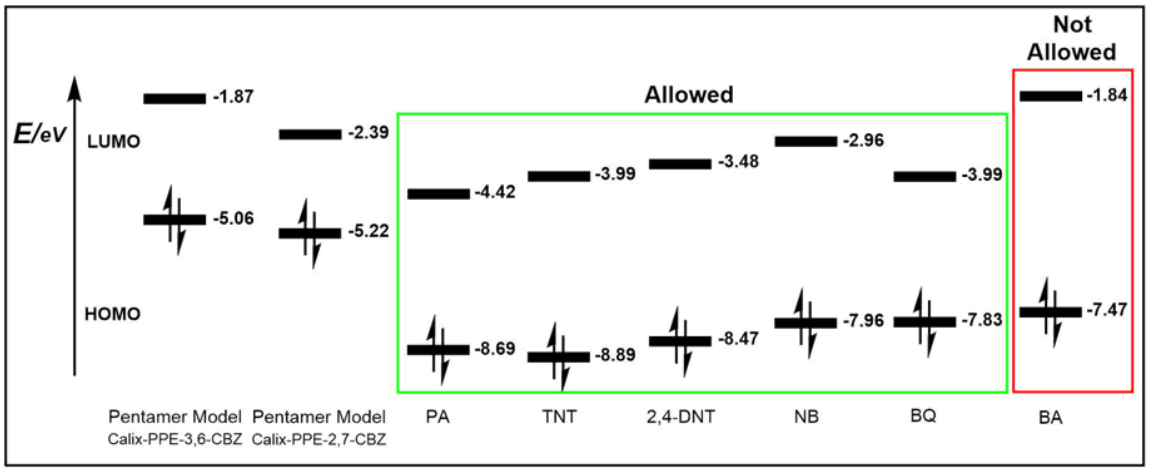

Figure S9. HOMO and LUMO energy levels of pentamer models of Calix-PPE-CBZs, NACs, BQ and BA. DFT calculations run at the B3LYP-D3/6-311+G(d,p) level of theory in vacuum [2,3].

Complex Model-Calix-2-CBZ-PA

Δ*E* = -84.0921 kJmol^{-1}

Complex Model-Calix-2-CBZ-TNT

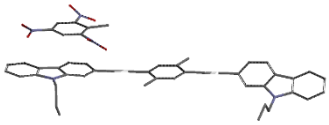

Δ*E* = -75.3203 kJmol^{-1}

Complex Model-Calix-2-CBZ-2,4-DNT

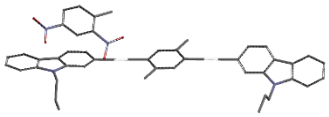

Δ*E* = -57.8634 kJmol^{-1}

Complex Model-Calix-2-CBZ-NB

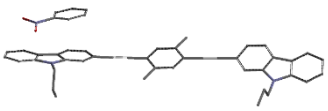

Δ*E* = -40.4957 kJmol^{-1}

Complex Model-Calix-2-CBZ-BQ

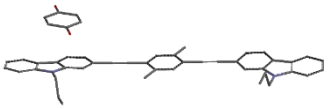

Δ*E* = -49.4434 kJmol^{-1}

Figure S10. Energy and geometry optimised structures of the complexes formed between Model-Calix-2-CBZ and various analytes. DFT calculations run at the B3LYP-D3/6-311+G(d,p) level of theory in vacuum [2,3]. Hydrogens omitted for clarity.

UV-Vis spectra of NACs

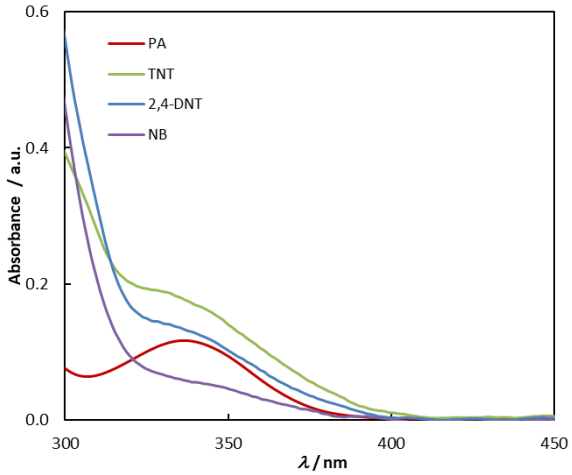

Figure S11. UV-Vis spectra of NACs (2.91 × 10^{-4} M, except for PA, 2.91 × 10^{-5} M, in $CHCl_3$).

Fluorescence titration data in solution

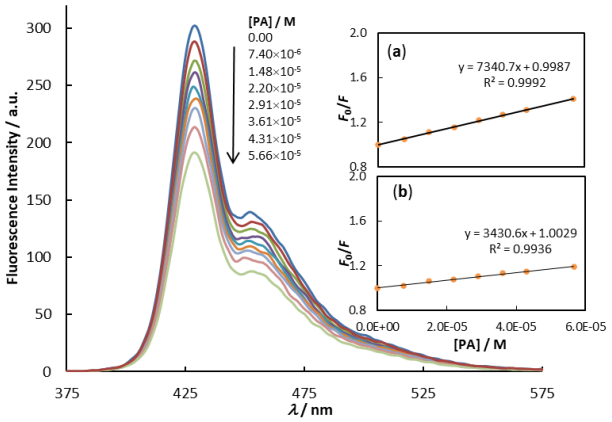

Figure S12. Emission spectra of Calix-PPE-2,7-CBZ (6.0×10^{-7} M in $CHCl_3$) after successive additions of PA (λ_{exc} = 360 nm). Inset: Uncorrected (**a**) and corrected (**b**) Stern-Volmer plots.

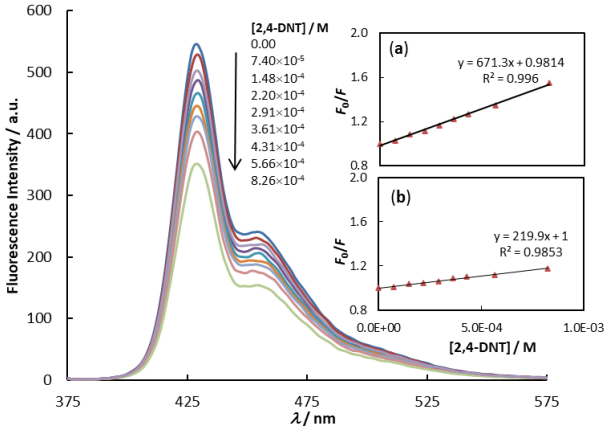

Figure S13. Emission spectra of Calix-PPE-2,7-CBZ (6.0×10^{-7} M in $CHCl_3$) after successive additions of 2,4-DNT (λ_{exc} = 360 nm). Inset: Uncorrected (**a**) and corrected (**b**) Stern-Volmer plots.

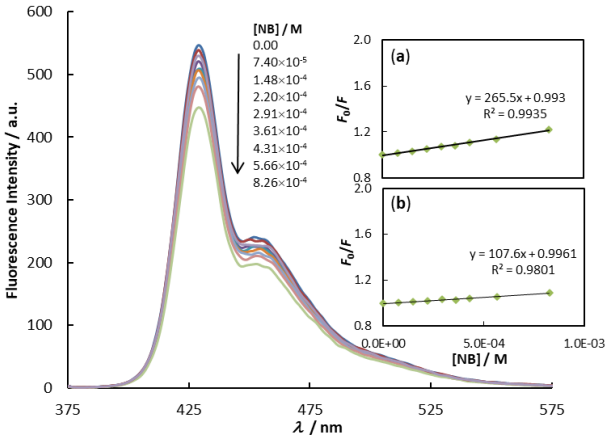

Figure S14. Emission spectra of Calix-PPE-2,7-CBZ (6.0×10^{-7} M in $CHCl_3$) after successive additions of NB (λ_{exc} = 360 nm). Inset: Uncorrected (**a**) and corrected (**b**) Stern-Volmer plots.

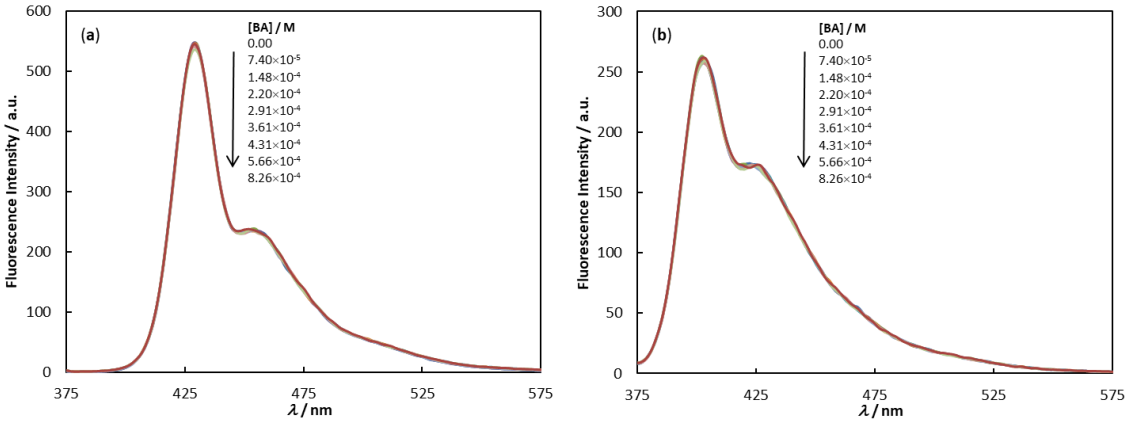

Figure S15. Emission spectra of Calix-PPE-2,7-CBZ (**a**) and Calix-PPE-3,6-CBZ (**b**) (6.0 × 10^{-7} M in $CHCl_3$) after successive additions of BA (λ_{exc} = 360 nm). The relative standard deviation (RSD) of emission intensities for 2,7-CBZ and 3,6-CBZ isomers were 0.69% and 0.83%, respectively.

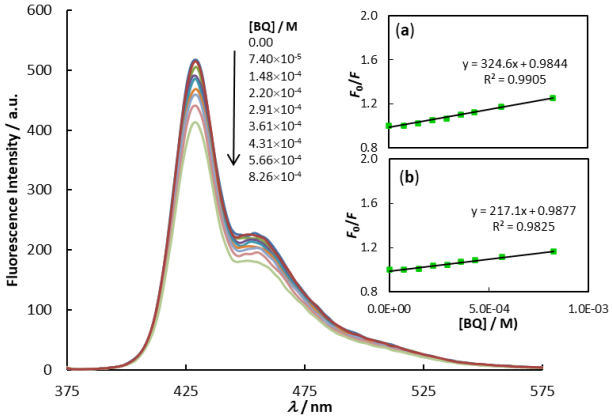

Figure S16. Emission spectra of Calix-PPE-2,7-CBZ (6.0 × 10^{-7} M in $CHCl_3$) after successive additions of BQ (λ_{exc} = 360 nm). Inset: Uncorrected (**a**) and corrected (**b**) Stern-Volmer plots.

Limit of detection of NACs in solution

The limit of detection (LOD) was calculated according to the 3σ IUPAC criteria [4], using the expression $LOD = \frac{3s_b}{S}$, where s_b is the standard deviation of emission intensity measurements (12 readings for each polymer at 6.0 × 10^{-7} M in $CHCl_3$; λ_{exc} = 360 nm), and S corresponds to the slope of the Stern-Volmer plot obtained for each NAC after correction. Results are depicted in Table S1.

Table S1. Limits of Detection of NACs

	PA / ppm	TNT / ppm	2,4-DNT / ppm	NB / ppm
Calix-PPE-2,7-CBZ	0.77	6.0	9.6	13.2
Calix-PPE-3,6-CBZ	1.64	15.3	17.9	29.4

Fluorescence titration data in solid state

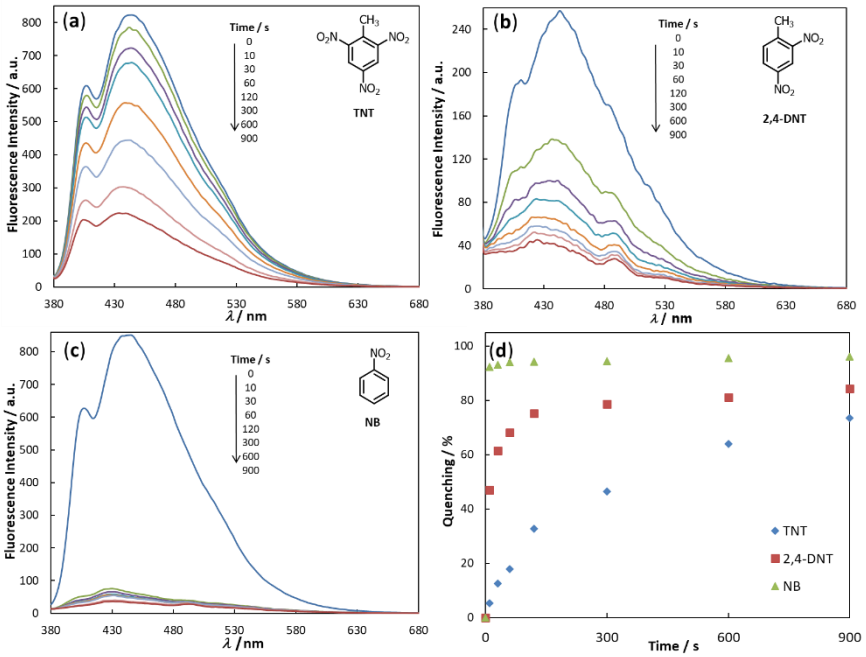

Figure S17. Time-dependent emission intensities (**a** to **c**) and fluorescence quenching efficiencies (**d**) of Calix-PPE-3,6-CBZ films (≈ 20 nm) after being exposed to saturated TNT (10 ppb) (**a**), 2,4-DNT (190 ppb) (**b**) and NB (318 ppm) (**c**) vapours at 25 °C (λ_{exc} = 360 nm).

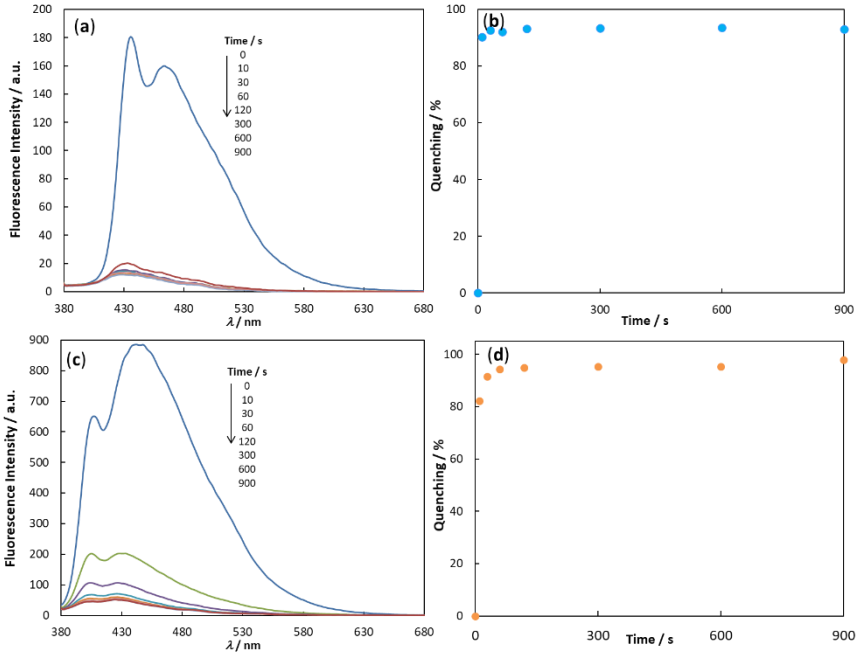

Figure S18. Time-dependent emission intensities (**a** and **c**) and fluorescence quenching efficiencies (**b** and **d**) of Calix-PPE-2,7-CBZ (**a** and **b**) and Calix-PPE-3,6-CBZ (**c** and **d**) films (≈ 20 nm) after being exposed to saturated BQ vapours (229 ppm) at 25 °C (λ_{exc} = 360 nm).

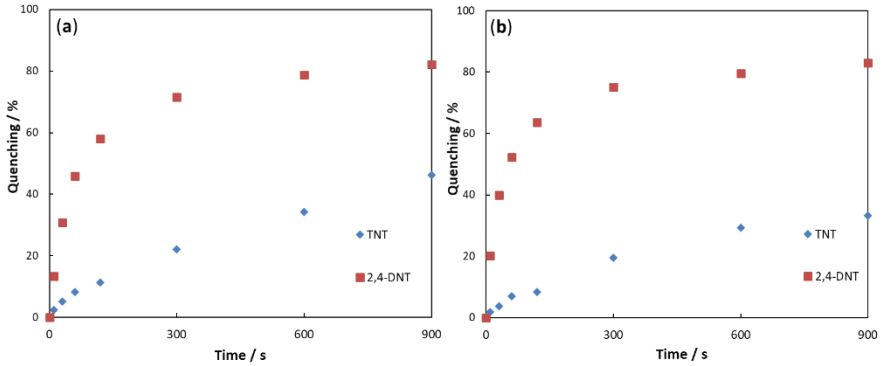

Figure S19. Fluorescence quenching efficiencies of TBP-PPE-2,7-CBZ (**a**) and TBP-PPE-3,6-CBZ (**b**) thin-films (≈ 15 and 50 nm, respectively) after being exposed to saturated TNT and 2,4-DNT vapours at 25 °C (λ_{exc} = 360 nm).

Fluorescence recovery data

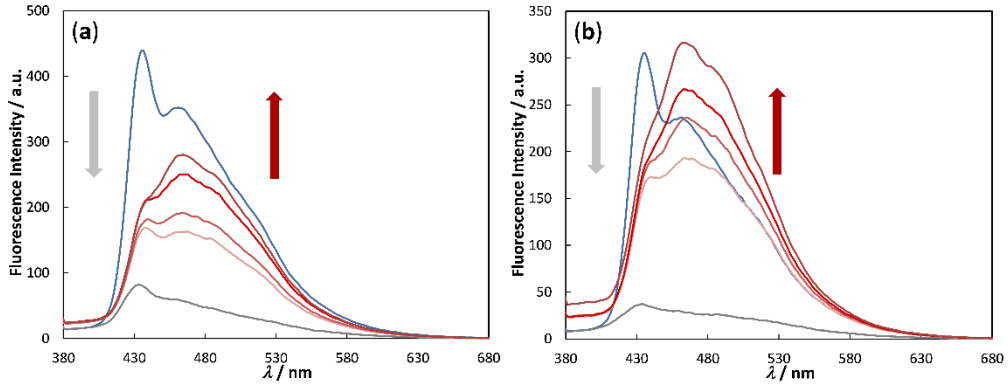

Figure S20. Quenching-recovery emission spectra of Calix-PPE-2,7-CBZ films (≈ 4 nm) before (blue line) and after (grey line) being exposed to saturated TNT (10 ppb) (**a**) and 2,4-DNT (190 ppb) (**b**) vapours, followed by exposure to hydrazine vapours (red lines; bottom to top) at various times (2, 5, 10 and 15 minutes); λ_{exc} = 360 nm, 25 °C.

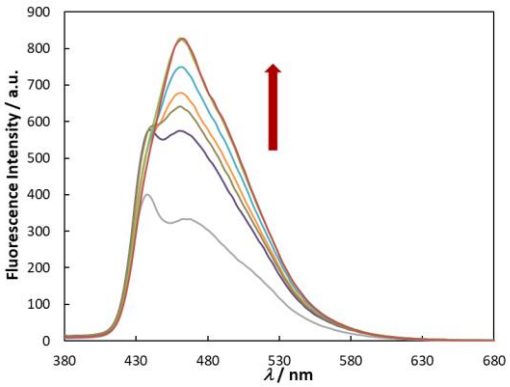

Figure S21. Emission spectra of Calix-PPE-2,7-CBZ film (≈ 4 nm) before (grey line) and after being exposed to saturated hydrazine vapours at various times (bottom to top; 2, 5, 10, 15, 20 and 25 minutes); λ_{exc} = 360 nm, 25 °C.

References

1. Barata, P.D.; Costa, A.I.; Prata, J.V. Calix[4]arene-carbazole-containing polymers: Synthesis and properties. *React. Funct. Polym*. **2012**, *72*, 627-634. https://doi.org/10.1016/j.reactfunctpolym.2012.06.006
2. Shao, Y.; Gan, Z.; Epifanovsky, E.; Gilbert, A.T.B.; Wormit, M.; Kussmann, J.; Lange, A.W.; Behn, A.; Deng, J.; Feng, X. et al. Advances in molecular quantum chemistry contained in the Q-Chem 4 program package. *Mol. Phys.* **2015**, *113*, 184–215, doi:10.1080/00268976.2014.952696.
3. *Spartan'18*, Wavefunction Inc., Irvine CA, USA, 2019.
4. Long, G.L.; Winefordner, J. D. Limit of Detection A Closer Look at the IUPAC Definition. *Anal. Chem*. **1983**, 55, 712A–724A. https://doi.org/10.1021/ac00258a724